

## **Solid-State Spiropyrans Exhibiting Photochromic Properties Based on Molecular Flexibility**

Lei Zhang,<sup>ab</sup> Yawen Deng,<sup>ab</sup> Yubao Tang,<sup>a</sup> Congxia Xie<sup>\*a</sup> and Zhongtao Wu<sup>\*a</sup>

<sup>a</sup>Key Laboratory of Optic-electric Sensing and Analytical Chemistry for Life Science, MOE; Shandong Key Laboratory of Biochemical Analysis; College of Chemistry and Molecular Engineering, Qingdao University of Science and Technology, Qingdao, 266042, PR China. E-mail: [xielongxia@126.com](mailto:xielongxia@126.com); [wuzhongtao@qust.edu.cn](mailto:wuzhongtao@qust.edu.cn)

<sup>b</sup>These authors contributed equally to this work.

### **1. General remarks**

### **2. Synthesis of SP<sub>4</sub>, SP<sub>8</sub> and SP<sub>12</sub>**

### **3. Characterizations of SP<sub>4</sub>, SP<sub>8</sub> and SP<sub>12</sub>**

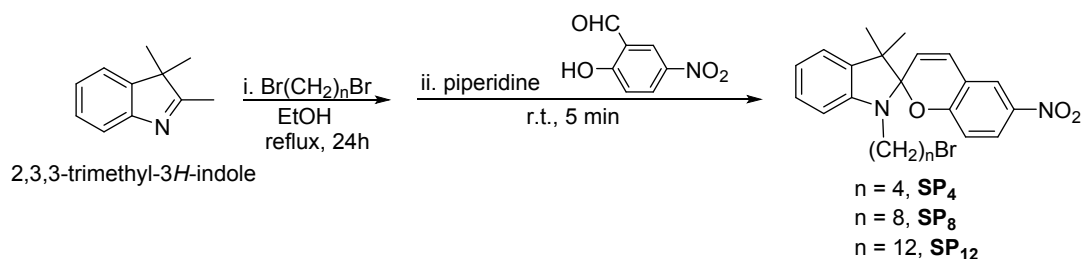
### **4. Characterizations of new compounds**

## 1. General remarks

$^1\text{H-NMR}$  and  $^{13}\text{C-NMR}$  spectra were recorded on a Bruker Avance 500 (500 and 125 MHz, respectively) with  $\text{CDCl}_3$  as a solvent. Chemical shifts were determined relative to the residual solvent peaks ( $\text{CHCl}_3$ ,  $\delta = 7.26$  ppm for  $^1\text{H NMR}$ ,  $\delta = 77.0$  ppm for  $^{13}\text{C-NMR}$ ). The following abbreviations are used to indicate signal multiplicity: s, singlet; d, doublet; t, triplet; m, multiplet; br, broad. Mass spectra were recorded on a Thermo Scientific LTQ Orbitrap XL machine. TGA was carried out using a Netzsch STA 449C thermal analyzer in a nitrogen atmosphere and with a heating/cooling rate of  $10\text{ }^\circ\text{C min}^{-1}$ . DSC was performed by a Netzsch DSC204F1 machine with a heating rate of  $10\text{ }^\circ\text{C min}^{-1}$ . POM was conducted on a Nikon ECLIPSE LV100NPOL machine with a computational controlled heating plate. SAXS was performed by employing a conventional X-ray source with radiation wavelength of  $\lambda = 1.54\text{ \AA}$ . The sample holder is a metal plate with a small hole (diameter  $\approx 0.5\text{ cm}$ , thickness  $\approx 0.5\text{ cm}$ ), where the X-ray beam passes through and the sample-to-detector distance was 20 cm. The scattering vector  $q$  is defined as  $q = 4\pi \sin\theta/\lambda$  with  $2\theta$  being the scattering angle. The UV-vis reflection spectra were recorded on a Perkinelmer Lambda750 machine. The UV-vis absorption spectra were recorded on a Shimadzu UV-2600 UV-vis spectrophotometer, and all the related studies were carried out on fast scan mode with slit widths of 1.0 nm, using matched quartz cells. All absorption scans were saved as ACS II files and further processed in OriginLab software to produce all graphs shown. The wavelengths of UV and vis photoirradiations are 365 nm ( $0.018\text{ W cm}^{-2}$ ) and 520 nm ( $0.068\text{ W cm}^{-2}$ ), respectively.

All starting materials, reagents and solvents were purchased and used without further purification. The pellets of **SP<sub>8</sub>** were prepared by heating the corresponding powder sample to isotropic liquid and then cooling to room temperature. Thin test sample of **SP<sub>8</sub>** was attached to the cell wall for UV-vis absorption spectra measurements via a heating-cooling process. One solely **SP<sub>8</sub>** pellet was used in Figure 4&5 for the whole photochromic and thermochromic studies. An observation that the absorption intensity of isotropic liquid mixture is little changed during the cooling process indicates (please see Figure S6): the absorption intensity change of different colored species should be caused by the SP-MC isomerization other than physical state change in this study. According to Lambert's law, the isomer ratio of **SP<sub>8</sub>:MC<sub>8</sub>** in the green isotropic liquid of Figure 4 is about 1.27:1, based on the absorption intensities of green liquid and purple pellet at 595 nm are 1.036 and 2.355. While, the ratio becomes to be 0.99:1 for the red isotropic liquid and red solid pellet in Figure 5, based on the absorption intensities of red pellet and purple pellet at 559 nm are 1.554 and 3.091. Please note this calculation is based on an assumption that purple pellet is composed of **MC<sub>8</sub>**.

## 2. Synthesis of **SP<sub>4</sub>**, **SP<sub>8</sub>** and **SP<sub>12</sub>**



**General procedure for the one-pot synthesis of spiropyrans:** to a solution of 2,3,3-trimethyl-3H-indole (0.5 mL, 3.14 mmol) in EtOH (20 mL) was added  $\text{Br}(\text{CH}_2)_n\text{Br}$  (3.14mmol, 1 eq), and the

resulting mixture was refluxed over 24 h. Then the reaction mixture was lowered down to the room temperature, which was followed by the addition of piperidine (0.31 mL, 3.14mmol, 1 eq) and 2-hydroxyl-5-nitrobenzaldehyde (3.14 mmol, 1 eq). The reaction was stirred over 5 min. Finally, the crude product was purified via a quick column chromatography to afford **SP<sub>4</sub>**, **SP<sub>8</sub>** and **SP<sub>12</sub>** as yellow solids.

**SP<sub>4</sub>**, **SP<sub>8</sub>**: **SP<sub>4</sub>** and **SP<sub>8</sub>** were obtained in 60% and 50% (an average number over several batches) yields respectively, and <sup>1</sup>H NMR spectra coincided with those reported in our previous results.<sup>[1]</sup>

**SP<sub>12</sub>**: Yield: 33%. <sup>1</sup>H NMR (500 MHz, CDCl<sub>3</sub>) δ 1.18 (s, 3 H), 1.23-1.28 (m, 17 H), 1.40-1.43 (m, 2 H), 1.55-1.64 (m, 2 H), 1.82-1.88 (m, 2 H), 3.08-3.20 (m, 2 H), 3.39-3.42(m, 2 H), 5.86 (d, *J* = 10.5 Hz, 1 H), 6.57 (d, *J* = 8.0 Hz, 1 H), 6.74 (d, *J* = 8.5 Hz, 1 H), 6.85-6.91 (m, 2 H), 7.08 (d, *J* = 7.5 Hz, 1 H), 7.18 (t, *J* = 7.5 Hz, 1 H), 8.00-8.02 (m, 2 H). <sup>13</sup>C NMR (125 MHz, CDCl<sub>3</sub>) δ 20.0, 26.2, 27.3, 27.4, 28.3, 28.9, 29.0, 29.5, 29.6, 29.6, 30.2, 32.9, 34.2, 43.9, 52.7, 106.8, 106.9, 115.6, 118.6, 119.3, 121.8, 122.2, 122.8, 125.9, 127.8, 128.1, 136.0, 141.0, 147.3, 159.8. HRMS (ESI) calcd. for C<sub>30</sub>H<sub>38</sub><sup>79</sup>BrN<sub>2</sub>O<sub>3</sub> [M – H]<sup>-</sup> 553.2071, found 553.2079.

### 3. Characterizations of **SP<sub>4</sub>**, **SP<sub>8</sub>** and **SP<sub>12</sub>**.

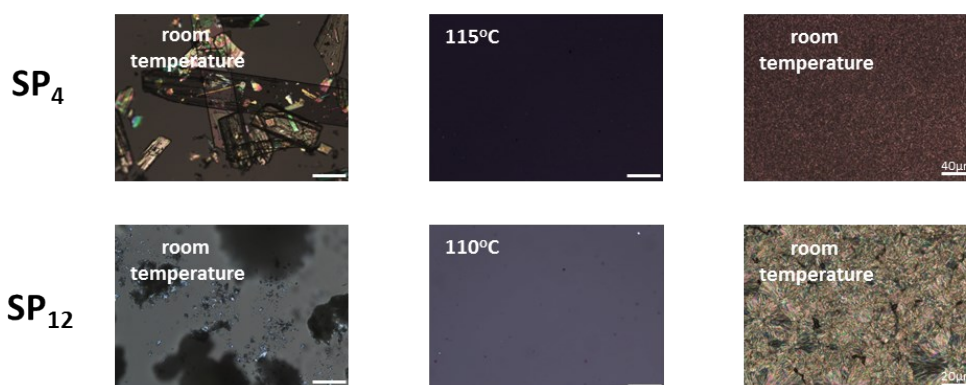


**Figure S1.** POM images of **SP<sub>4</sub>** and **SP<sub>12</sub>** under room temperature→their clearing points→room temperature. For the POM images of **SP<sub>8</sub>**, see: Figure S3 in the supporting information, and Figure 4a-insets in the main text.

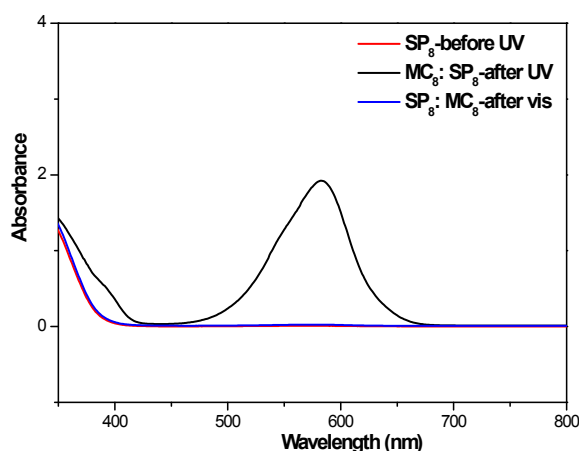


**Figure S2.** UV-vis absorption spectra of **SP<sub>8</sub>** in ethyl acetate solution ( $9 \times 10^{-5}$  mol L<sup>-1</sup>).

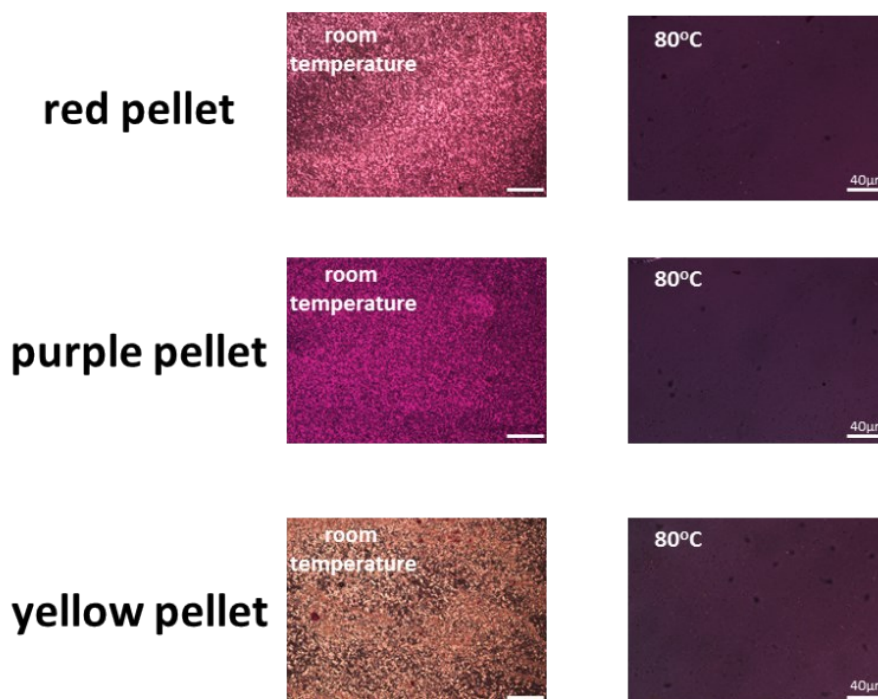


**Figure S3.** POM images of red pellet (**J-MC<sub>8</sub>-II&J-SP<sub>8</sub>-III**), purple pellet (**J-MC<sub>8</sub>-II&J-MC<sub>8</sub>-III**) and yellow pellet (**J-SP<sub>8</sub>-II&J-SP<sub>8</sub>-III**) under room temperature and at 80 °C. These images indicate that the ordered structures of red pellet, purple pellet and yellow pellet at room temperature become isotropic at 80 °C.

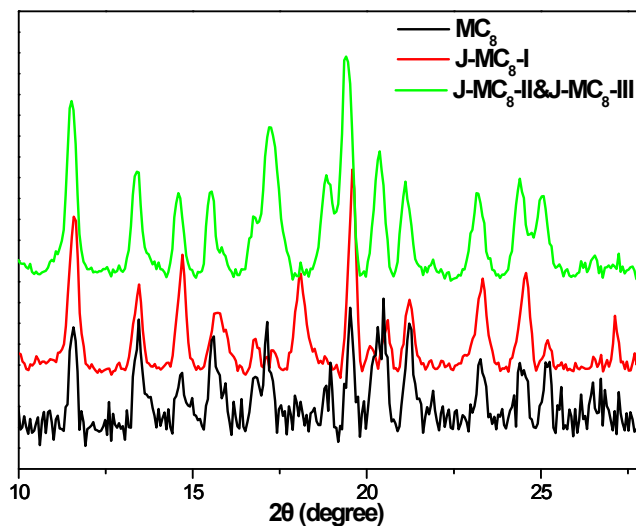


**Figure S4.** Comparison on SAXS spectra of the purple pellets **MC<sub>8</sub>**, **J-MC<sub>8</sub>-I** and **J-MC<sub>8</sub>-II&J-MC<sub>8</sub>-III**. **J-MC<sub>8</sub>-II&J-MC<sub>8</sub>-III** and **J-MC<sub>8</sub>-I** are showing similar SAXS profiles, indicating that they are in similar molecular arrangement (both in J-aggregation arrangement, as discussed in manuscript). While, with higher stacking intensity the alternating **J-MC<sub>8</sub>-II** and **J-MC<sub>8</sub>-III** arrangement also results in the difference on its SAXS profile from that of **J-MC<sub>8</sub>-I**.

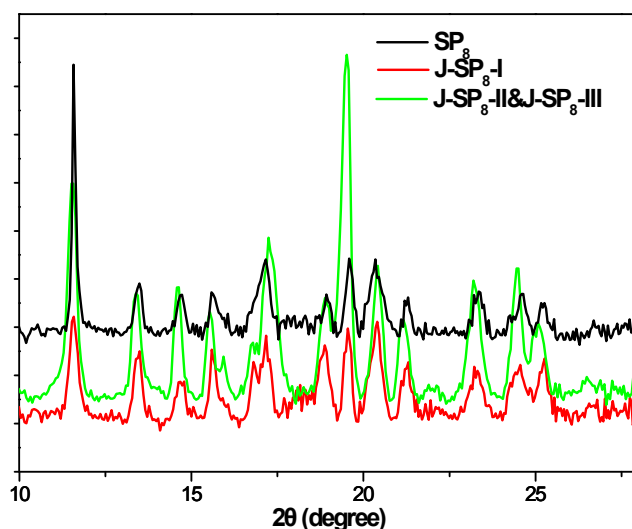


**Figure S5.** Comparison on SAXS spectra of the yellow pellets  $SP_8$ ,  $J-SP_8-I$  and  $J-SP_8-II&J-SP_8-III$ .  $J-SP_8-II&J-SP_8-III$  and  $J-SP_8-I$  are showing similar SAXS profiles, indicating that they are in similar molecular arrangement (both in J-aggregation arrangement, as discussed in manuscript). While, with higher stacking intensity the alternating  $J-SP_8-II$  and  $J-SP_8-III$  arrangement also results in the difference on its SAXS profile from that of  $J-SP_8-I$ .

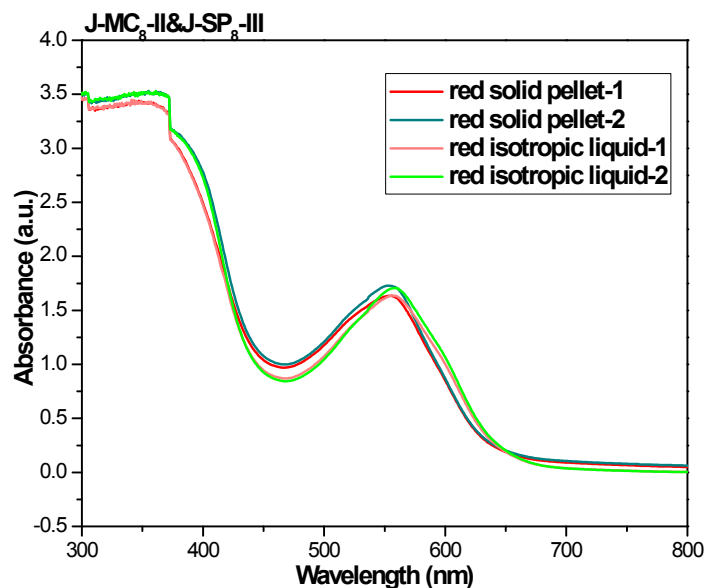


**Figure S6.** UV-vis absorption spectra changes of  $J-MC_8-II&J-SP_8-III$  under  $80^\circ C$  and room temperature in two cycles. The same absorption intensity between red solid pellet and red isotropic liquid indicates that  $J-MC_8-II$  don't give  $MC \rightarrow SP$  isomerization during the cooling process. A slight blue shifted absorption change of red solid pellet compared to isotropic liquid is caused by the more compact molecular arrangement.

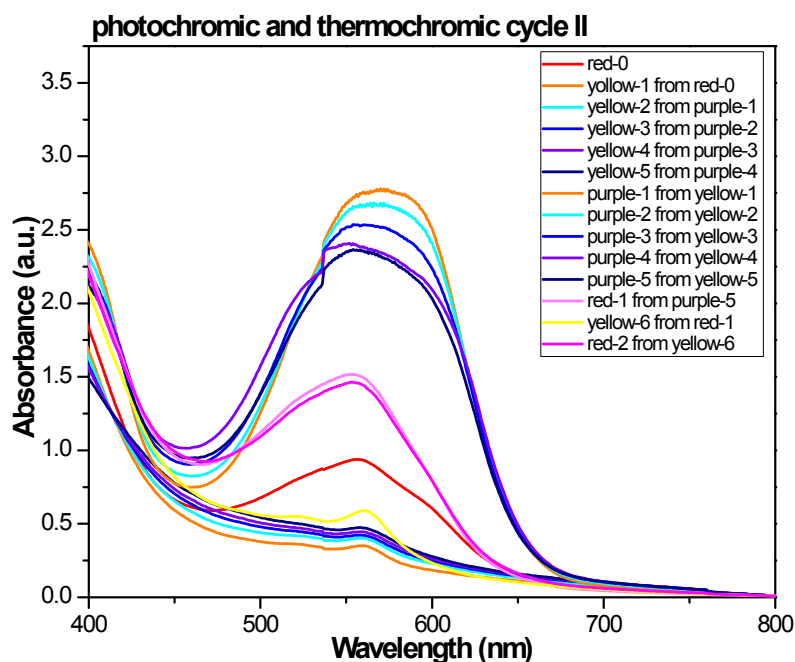


**Figure S7.** Fatigue resistance tests on  $SP_8$  pellets in photochromic and thermochromic cycle II. During the tests, red, purple and yellow colors could be well reproduced, with no color fading by naked eyes. The little decreased absorption intensity of purple pellet and the little increased absorption intensity of yellow pellet in the first few cycles would be caused by the slight intermolecular packing density change of purple pellet and yellow pellet during the  $SP \rightleftharpoons MC$  isomerization. And the almost same absorption intensity of purple pellet in cycle 4 and 5 indicates the solid-state  $SP_8$  reaches the “final stable” packing density. The absorption density change of red pellet from red-0 to red-1&2 is caused by the sample flow during the heating process, since the measured sample is attached to the cell wall.

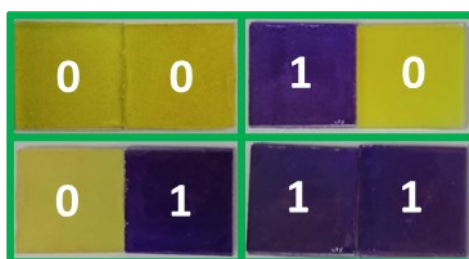


**Figure S8.** A binary-codes system based on  $SP_8$  and  $MC_8$ . Here, we define yellow = 0 and purple = 1, which gives 4 different codes.



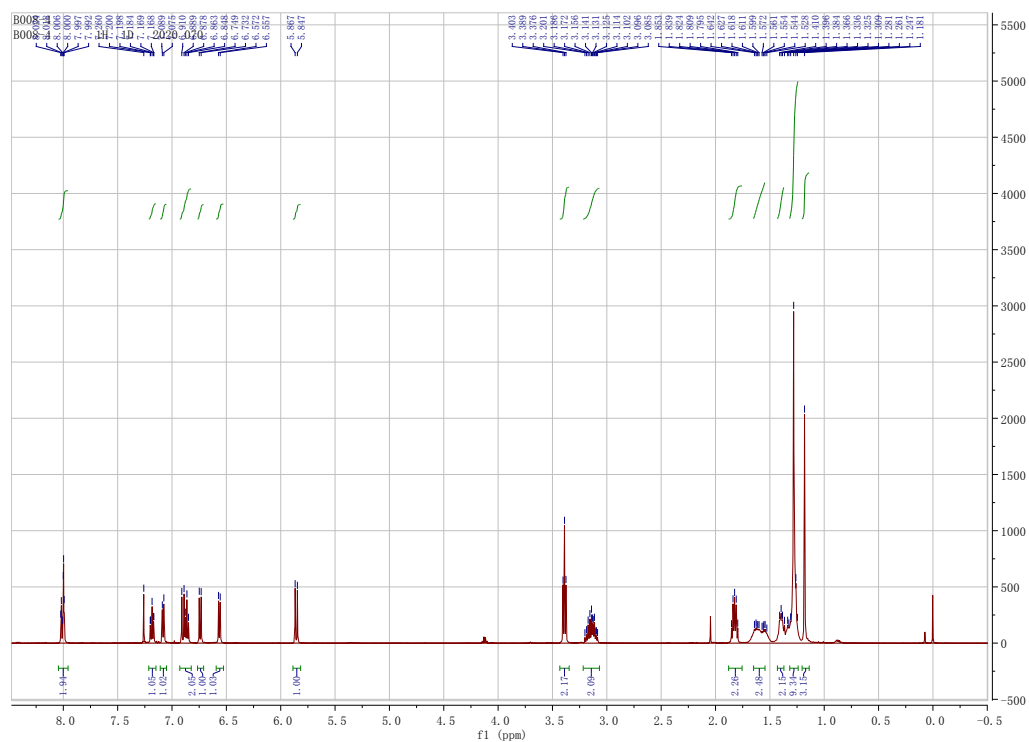


Figure S11. <sup>1</sup>H NMR of SP<sub>8</sub> after UV-vis photoirradiations over 15 times.

#### 4. Characterizations of new compounds

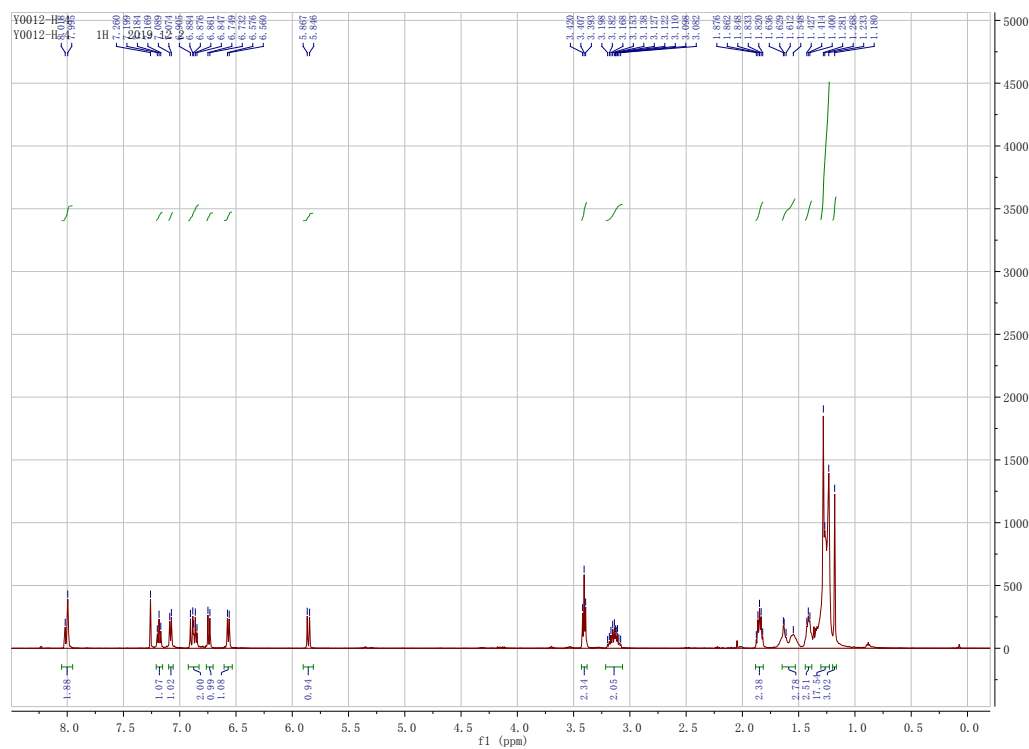


Figure S12. <sup>1</sup>H NMR of SP<sub>12</sub>.

